Seismic Fragility Analysis of Torsionally-Coupled Steel Moment Frames Against Collapse

Mesr Habiby, Y.[1] and Behnamfar, F.[2*]

[1] M.Sc., Department of Civil Engineering, Isfahan University of Technology, Isfahan, Iran.
[2] Professor, Department of Civil Engineering, Isfahan University of Technology, Isfahan, Iran.

© University of Tehran 2023

ABSTRACT: In this study, nonlinear dynamic response of 4, 7, and 10-story moment frame steel structures is investigated under seismic ground motions. An incrementally increasing intensity is accounted for to evaluate the collapse fragility curves of the same buildings under different values of torsional eccentricity. The site soil of the buildings is assumed to be composed once of a firm and then of a soft soil. As a distinction of this study, the realistic maximum possible value of eccentricity ratio for moment frames, including both stiffness and mass eccentricities, is shown to be 10-15% that is much less than peak values of the past studies. Because of the three-dimensional aspect of the study, the eccentricity is selected to be bi-directional and the horizontal components of the earthquake motion are applied concurrently. It is exhibited that while torsional eccentricity lowers the median collapse probability of the studied buildings, it does not have a sensible effect up to the eccentricity ratios not larger than 10%. Besides, the taller structures on the firm soil are affected more strongly from torsional eccentricity, as the median collapse acceleration decreases up to 46% for the 10-story building suffering from 15% eccentricity ratio on the firm soil.

Keywords: Collapse, Eccentricity, Seismic Fragility, Steel Structure, Torsion.

1. Introduction

Buildings having torsional eccentricity in plan have been known to suffer more from earthquake damage. The horizontal displacement of the plan of a torsionally-coupled building is not uniform during an earthquake even if the story diaphragms are rigid. This is turn results in accumulation of ductility demands at the soft side, i.e. part of the plan where the peak horizontal displacement happens. Then, seismic damage begins to develop at a large extent from the same location instead of being uniformly distributed among all resisting elements, at much smaller intensity.

In response to the above negative observations on seismic torsional response, strict regulations have been developed in building codes to lower torsional eccentricity and its consequences. For instance, ASCE 7-16 (2016) sets certain constraining regulations to amplify torsional demands. When the torsional

---

* Corresponding author E-mail: farhad@cc.iut.ac.ir

eccentricity exceeds a predefined threshold, it necessitates the spectral analysis for critically torsional buildings, and prohibits designing buildings with large eccentricities for more important building in highly seismic areas (ASCE/SEI 7-16, 2016). The point here is that abiding by these regulations results in buildings with much less eccentricities than what appears in the initial architectural drawings of the building. Then, assuming extremely large values of the eccentricity ratio in research studies is only of academic value.

Due to its importance, many researchers have embarked on the effects of torsional response of building in highly seismic areas. More than 70 of these studies, performed between 1990-2020, have been identified and reviewed in a relevant work (Habiby, 2020). Only a number of the more important works are mentioned here to form a general idea.

Mazzolani and Piluso (1996) and Gioncu and Mazzolani (2010) compiled the temporary knowledge on earthquake engineering and design of steel structures to withstand earthquakes in the form of two interesting textbooks. On critical examination of the Eurocode 8, Elghazouli (2010) assessed the seismic regulations of steel structures, Ferraioli et al. (2014) evaluated the appropriateness of the code-based behavior factor for steel structures, and Landolfo (2018) introduced the ongoing trends of the code improvement regarding seismic design of steel structures.

Patel et al. (2016), Xu et al. (2018), Dehghani and Soltanimohajer (2022), Zeng et al. (2022), and Ashwini and Stephen (2022) are among the authors who worked on developing the seismic fragility of frame structures considering various parameters including engineering demand parameters, height of the building, and supplemental damping.

Chen and Collins (2001) modified the method developed by Collins et al. (1996) for reliability-based seismic design of torsional structures. According to their study, the only necessary change in the

previous process was the use of 3D pushover analysis to calibrate the parameters of the equivalent Single Degree Of Freedom model (SDOF), and the general form of the design equations did not change. The results indicated that the uncertainty amplification in the SDOF model considering the torsion was not significant. It also seemed that the design parameters were not sensitive to changes in the statistical values used to quantify the approximate nature of the SDOF method. The reason for this was that the other two sources of uncertainty (seismic hazard and site soil effects) dominated the uncertainty of the analysis and design values. However, results of the study need further investigation, because it was based on very simple analytical models and some restrictive assumptions.

Puppio et al. (2017), Seo (2018), Moon et al. (2018), Anvarsamarin et al. (2020), and Razmkhah et al. (2021) determined the seismic fragility curves by accounting for torsional irregularity in plan of the buildings. Generally, they concluded that torsional irregularity increases the seismic fragility to a considerable level.

Marušić and Fajfar (2005), evaluated the linear and nonlinear seismic response of asymmetric five-story steel buildings under bi-directional excitation. Asymmetric buildings were created with the eccentricity of the mass in both main directions. In torsionally stiff structures, the nonlinear torsional response was qualitatively similar to the linear response, except for the stiff edge in the strong direction, i.e. the direction in which the component with higher peak ground velocity was applied to the structure. Generally, formation of the plastic hinges reduced the torsional effect. It was concluded that displacement of the mass center in the asymmetric building and the symmetrical building was approximately equal. Amplitude of the displacement calculated by linear analysis was a proper approximation for the corresponding value in the nonlinear region. Any desirable torsional effect on the

stronger edge of the torsionally stiff structure, i.e. a displacement reduction relative to the symmetric structure, was due to linear analysis, and this effect might be eliminated in nonlinear analysis.

De Stefano and Pintucchi (2008) reviewed the research works on seismic behavior of torsionally-coupled buildings since 2002 having different structures. They examined the main features of the seismic response of irregular buildings and provided certain recommendations and future directions. Aziminejad and Moghadam (2010) evaluated the seismic performance of asymmetric single-story buildings under near-field and far-field earthquakes based on the fragility concept. They showed that in general, the optimal location of centers of stiffness and strength was a function of the characteristics of ground motion and nonlinear responses of structure. In their study, by evaluating the nonlinear response of one-story building models with a wide range of rotational to lateral frequency ratios, the optimal location of these centers was investigated. Diaphragm rotation, interstory drift, hinge rotation and ductility demand have been selected as damage indices. Results showed that the proper configuration of structural centers in a torsionally stiff building mainly depended on the selected demand parameter. For a specific demand parameter, such a proper configuration could lead to convergence of damage probability to that of the symmetrical building. Therefore, by identifying the critical demand parameter for a particular case, it was possible to detect the suitable arrangement of the centers and by rearranging the centers accordingly, the negative effects of asymmetry could be avoided.

Bensalah et al. (2013) studied the effect of torsion on the behavior of three-story reinforced concrete structures with rigid slabs. Uncertainty of input parameters such as Arias intensity, Peak Ground Acceleration (PGA), principal period and outputs such as interstory drift and torsional eccentricity were investigated. Time history and pushover analyses were performed under 116 earthquake records. They concluded that in low-rise multistory structures, the torsional response during an earthquake depended on many factors and the most effective parameter was the PGA with the highest correlation.

In the study implemented by Fujii (2014), a pushover-based method was proposed to estimate the maximum seismic response of an asymmetric building under an excitation with an arbitrary angle of incidence. The specifications of the two independent SDOF models were determined according to the main direction of the first modal response in each nonlinear phase, unlike the usual method that uses a fixed direction based on the linear mode shape. In the numerical example, six 4-story torsionally stiff buildings under seismic excitations at various angles were subjected to nonlinear dynamic. The results showed that the maximum displacement response of the soft edge of the torsionally stiff building obtained from the proposed method had a good accuracy. Orthogonality of the main directions of the modal response of the first and second modes of the structure was true for torsionally stiff structures, but in the torsionally flexible structures these responses were not independent of each other.

Sharifi and Sakulich (2014) studied the effects of torsion on the nonlinear response of steel structures. A number of 4, 8 and 12-storey steel moment frame structures were considered with various eccentricities. Intensity of eccentricity was an important parameter that changed the degree of participation of different transition and rotation modes in the total response. It was observed that increasing eccentricity of the structures increased participation of the floor rotation in the total response. In addition, in torsionally flexible structures when the first or second mode was mainly composed of torsional vibration, the rate of floor rotation participation could be even higher. This indicated that the torsional

mode of the structure must be controlled, by means of damping systems and control devices, to effectively reduce lateral displacement.

In the study by De Stefano and Mariani (2014) the positive and negative aspects of different analysis methods appropriate for torsional structures were described and recommendations for improving the existing building codes were proposed.

DeBock et al. (2014) investigated the importance of seismic design accidental torsion criteria of ASCE 7-16 on the collapse capacity of RC buildings with ordinary and special moment frame lateral systems. Their study, which was performed using 22 pairs of earthquake records, showed that the requirements of accidental torsion do not have much effect on increasing the collapse capacity of buildings. For example, according to their results, these criteria improve only the collapse behavior of buildings located in moderate seismic regions suffering from Torsional Irregularity Ratio (TIR) greater than 1.4 and buildings located in high seismic regions with TIR greater than 1.2.

In a case-study presentation, Ferraioli (2015) provided a comprehensive seismic performance assessment of an irregular hospital building, embarking on its nonlinear response and the main involving factors.

Manie et al. (2015) probabilistically studied the collapse behavior of low-rise asymmetric plan buildings under bi-directional ground motions. The nonlinear model of the structural members included concentric inelastic rotational springs at the ends of the otherwise elastic members. Degradation of stiffness and strength was included in the nonlinear springs. The torsional eccentricity was made by dislocating the center of mass in one direction. It was concluded that by increasing the eccentricity, a smaller margin of safety is resulted against seismic collapse. For values of the eccentricity ratio over 20%, the safety margin fell below the minimum value required for fulfilling the

life safety performance level. They observed a decreasing trend of the safety margin with increasing the number of stories of the studied buildings.

Badri et al. (2016) studied the effect of deteriorating parameters on the collapse capacity of asymmetric low-rise buildings. The studied five-story buildings were of RC moment frame type and had a one-way mass eccentricity in the plan. One-directional far-field ground motions was selected for dynamic analysis. Buildings were divided into two groups: torsionally stiff and torsionally flexible. Torsionally stiff building had their periods of the translational mode to be significantly larger than their period of torsional mode in opposite to the torsionally flexible buildings. Results of the analysis showed that increasing the torsional eccentricity of ductile moment frames can slightly increase or even reduce the collapse probability of structures, which was due to stiffer torsional behavior of the studied structures. Also, as the mass eccentricity increased, the uncertainty of modeling parameters had a smaller effect on the safety margin of collapse.

Han et al. (2017) investigated the nonlinear seismic response of special steel moment frame buildings having torsional irregularity and evaluated the effects of torsional regulations of the sample building codes on the collapse safety margin of such structures. They displaced one of the moment frames at predefined values to impose torsional response due to stiffness eccentricity. It was shown that torsional irregularity increases the collapse probability in general. They developed a method for limiting the drift demand of stories such that the collapse probability of unsymmetric structures equaled that of their regular counterparts.

Eivani et al. (2018) studied the seismic behavior of asymmetric single-story structures with flexible diaphragms having different configurations of centers of mass, stiffness and strength. Effect of asymmetry on diaphragm deformation as well as effect

of diaphragm flexibility on seismic demands were studied. The optimal configuration of centers of mass, stiffness and resistance was also investigated to limit the critical engineering demand parameters. The results showed that the predominant shear deformation of the diaphragms depended on both structure asymmetry and flexibility of the diaphragm. It was also found that the proper configuration of the centers in torsionally stiff structures depended on the level of flexibility of diaphragm in addition to the intensity of earthquake and the engineering demand parameters.

Hentri et al. (2018) evaluated the seismic behavior of asymmetric RC structures using a Displacement-based Adaptive Pushover (DAP) method. Fragility curves were determined for various performance states. The results indicated that height of the asymmetric structures significantly affected their response and the strength and stiffness of the structures were a function of their slenderness ratio, especially in taller buildings. It was concluded that in asymmetric structures, more displacement and ductility capacities were required to achieve the same behavior as the symmetrical structures.

Das et al. (2021) examined an exhaustive number of studies in the literature of asymmetric and irregular structures. Because of the varied nature of the results, the guidelines are not yet well developed. In fact, distinctions in results observed even in the behavior of a single-story asymmetric structure, especially for regulation of inelastic behavior, is a major obstacle to reach the comprehensive guidelines.

Hwang et al. (2021) developed a machine learning-based methodology for reliably predicting the seismic response and structural collapse classification of RC buildings by using four component- and system-level modeling uncertainties. The RC beam modeling parameters (i.e., plastic deformation properties) of low- to mid-rise structures were the primary predictors of seismic response due to capacity design rules. In addition, models that ignore the uncertainties of the structural modeling-related parameter seem to underestimate collapse risk of low- to mid-rise RC buildings.

Moradi et al. (2022) evaluated the collapse probability of a 4-Story RC frame under post-earthquake fire scenario. The results showed that increasing PGA makes the building behavior more critical and decreases collapse time in these buildings under post-earthquake fire loading.

Tavakoli et al. (2022) investigated outrigger braced system placement effect on seismic collapse probability of tall buildings. For this goal, two structures of 50 floors were chosen. The results showed that the placement optimization of outrigger braced system enhances all structural parameters and decreases the collapse probability. Furthermore, the fragility curves derived from plastic strain energy were quite similar to the fragility curves generated from the story drifts.

Kazemi and Jankowski (2023) proposed machine learning-based algorithms to predict seismic limit-state capacity of steel MRFs considering soil-structure interaction. This study enhanced data-driven decision method in python software, known as supervised machine learning algorithms, to find median IDA curves for predicting seismic limit-state capacities. The results of the analysis confirmed that there is no specific model for anticipating the IDA curves of structures; therefore, the best algorithms to diminish high computational costs were proposed.

It is observed by the above literature review that the nonlinear seismic response of torsionally eccentric steel structures is yet to be fully known. Especially, probabilistic assessment of such a behavior and evaluation of the seismic safety margin of the steel moment frames to the extent of building code modification need much more study. This is an important aspect that the related literature lacks enough consideration. The present study is a step toward filling this gap by examining the

probabilistic features of the seismic response of torsionally-coupled buildings. Moreover, it is aimed to probabilistically find the threshold of the eccentricity ratio over which the building code should beware the designer to be concerned over the consequences. Obviously, vital to such a study is taking realistic assumptions for the eccentricity ratio of the centers of mass and stiffness. This study critically touches this very important point to find the reliable range of the ratio to make the findings meaningful. In most of the past studies, the collapse behavior of asymmetric buildings has been investigated assuming irregularity of mass in the plan. It also seems that the assumed values of eccentricity in previous research works has been sometimes much higher than the possible values. In the present study, first, the maximum feasible values of the eccentricity of torsionally-coupled buildings are determined and then the safety margin against seismic collapse of such buildings is evaluated. The wider range of cases studied, leads to more comprehensive results. Here, low and medium rise steel structures having 4, 7, and 10 stories consisting of special moment frames are studied using Incremental Dynamic Analysis (IDA) to draw their fragility curves. When designing these structures, a firm and then a soft soil site are considered. In nonlinear analysis, different values of mass eccentricity in a stiffness-eccentric plan are considered. Variation of the collapse safety margin and the median spectral acceleration with the eccentricity

ratio, building height, and the soil type are discussed.

2. The Realistic Range of Eccentricity

This research study is recognized from the majority of the similar studies in the past by the fact that it evaluates the response of multistory buildings having conventional beams, columns, and diaphragms in contrast to the ones embarking only on mathematical models of real buildings by working only with stiffness and mass parameters. Therefore, it is necessary beforehand to configure the arrangement of the building frames to arrive at a certain value of eccentricity. In the past studies, values of eccentricity ratio, i.e. distance of the mass and stiffness (as opposed to strength) centers divided by the plan dimension along a major axis, up to values over 30% have been assumed. It is shown here that such large eccentricities are not possible in practice and a more realistic bound is derived. Three critical examples are considered as follows. It is to be noted that only conceptual facts are important here. Then, extensive details of the example buildings, designed based on AISC 360-16 (2016), are not given to save space for the next parts of the paper.

2.1. Example 1
   In this example a mass-eccentric moment frame building is considered (Figure 1).
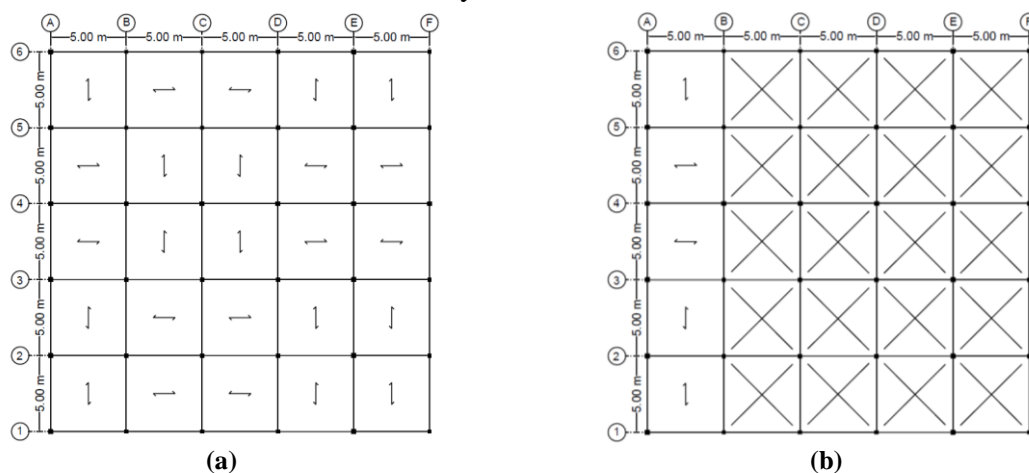

Fig. 1. The story plan considered in Example 1: a) Regular case; and b) Irregular case

According to Figure 1b, as an extreme case, it is assumed that a large part of the plan (indicated by crosses) is void. On the remaining part, a large live load of 12 KN/m^2 is applied that can be due to a heavy storage area. The building consists of 5 stories. At the first step, for modeling using a commercial design program, identical frames are considered throughout the plan. The mass eccentricity ratio along the y-axis is calculated to be about 34%. Then the building is analyzed assuming a highly seismic zone in ASCE 7-16. For such a large torsional eccentricity, the frames under the covered part of the plan undergo much larger displacements than the opposite frames and accept amplified lateral loads when using spectral analysis. After the first round of analysis and design, the mentioned frames prove to need larger sections than the other frames. Then the eccentricity ratio reduces to about 16% based on stress limitation and only 5% based on both stress and drift limitations. For the regular building, the beams sections emerge to vary from IPE160 to IPE360. The columns are 180×20 to 320×25 boxes. In the irregular building, designed sections vary from IPE160 to IPE400 for the beams and from 180×20 to 380×25 boxes for the columns.

2.2. Example 2

In this example, the torsional eccentricity originates from non-uniform arrangement of uniformely-sectioned steel moment frames (Figure 2).

It is perceived that locating two frames at such a close proximity in a direction having only three frames is not conventional. However, the example goes on to study a very extreme case to reach to an upper bound of eccentricity.

Using conventional dead and live loads and a highly seismic zone within ASCE 7-16, the frames are designed according to AISC 360-16. Before the first round of analysis, by assuming uniform stiffness for the frames, the eccentricity ratio emerges to be 17%. After finalizing the design process through a few iterations, the eccentricity ratio reduces to about 5%. In this example, for the regular building case, the beam sections appear to vary from IPE240 to IPE360 and the columns are 180×20 to 300×20 boxes. In the irregular building, sections vary from IPE240 to IPE400 for the beams and from 240×20 to 400×40 boxes for the columns.

As the above two examples prove, real contemporary seismic design of moment frames, even in the most extreme cases, does not allow the final torsional eccentricity to be larger than, perhaps, about 10-15%. Assuming larger eccentricities, therefore, will not have a considerable practical value.
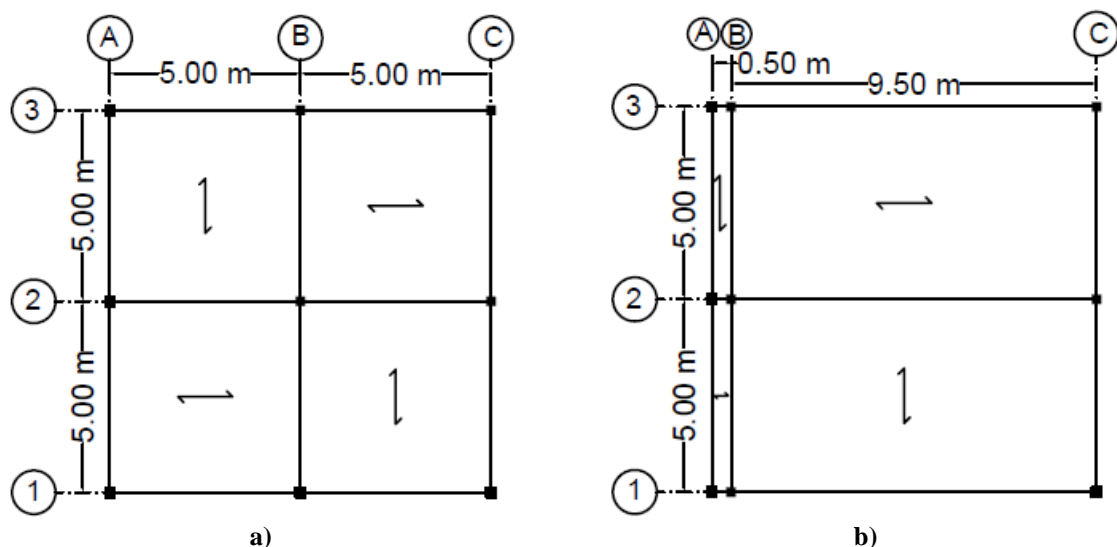

a)   b)
Fig. 2. Arrangement of the moment frames in Example 2: a) Regular case; and b) Irregular case

2.3. Example 3

In order to generate high torsional eccentricities, braces that have more stiffness than moment frames can also be used (Figure 3). Thus, in the third example, one-way eccentricity is made in a building equipped with a dual lateral load bearing system. The plan and other specifications are similar to Example 2. In the mentioned building, the B axis is shifted to the west side while it is braced between 1-2 axes. The mass distribution on the plan is considered to be uniform. By choosing uniform initial sections for the members without regard for the inherent torsion (with member section being similar to a regular building), the one-way eccentricity ratio reaches to 38%. After the final round of analysis and design including abiding by the weak beam-strong column requirement, the dual system specific controls and drift limitation, eventually the eccentricity ratio only decreases to 35%. In this example, for the regular building case, the beam sections appear to vary from IPE240 to IPE300, the columns are 180×20 to 240×20 boxes and the braces are 120×20 box. In the irregular building, sections vary from IPE160 to IPE360 for the beams, from 220×20 to 340×25 boxes for the columns and 120×10 box for the braces.

By designing the structure with a dual system of moment frame and bracing in one direction, two results can be obtained in comparison to the previous examples:

a) In structures with irregularity due to displaced braced frames, after finalizing the design process, the stiffness center shifts only slightly and the change in the initial value of eccentricity is not significant. On the opposite, in structures with irregularity due to displaced moment frames, the value of eccentricity is extremely reduced by the design process. The reason for this is dependence of stiffness of moment frames on the dimensions of the beams and columns sections, while for the braced frames, stiffness of the braced bays is normally much higher than the otherwise moment frames.

b) In the irregular structures with the dislocated braced frames, the process of repetitive analysis and design has a small effect on the position of the stiffness center because of the concentrated large stiffness of the braced bays.

Then, unlike most of the previous studies where virtual structures with deliberate eccentric arrangement of members were studied without performing actual design of the buildings for those presumed eccentricities, any kind of the assumed eccentricity should be regarded in design and proportioning of the members to arrive at a final reduced eccentricity. This important fact is fulfilled in this study.

3. Introducing the Studied Buildings

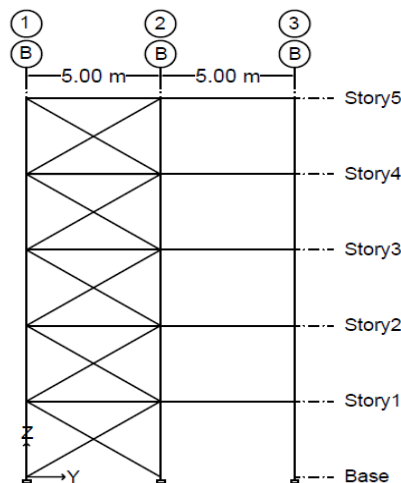Configuration of the buildings selected for the current study is shown in Figure 4.

Fig. 3. Braced frame of the building in Example 3
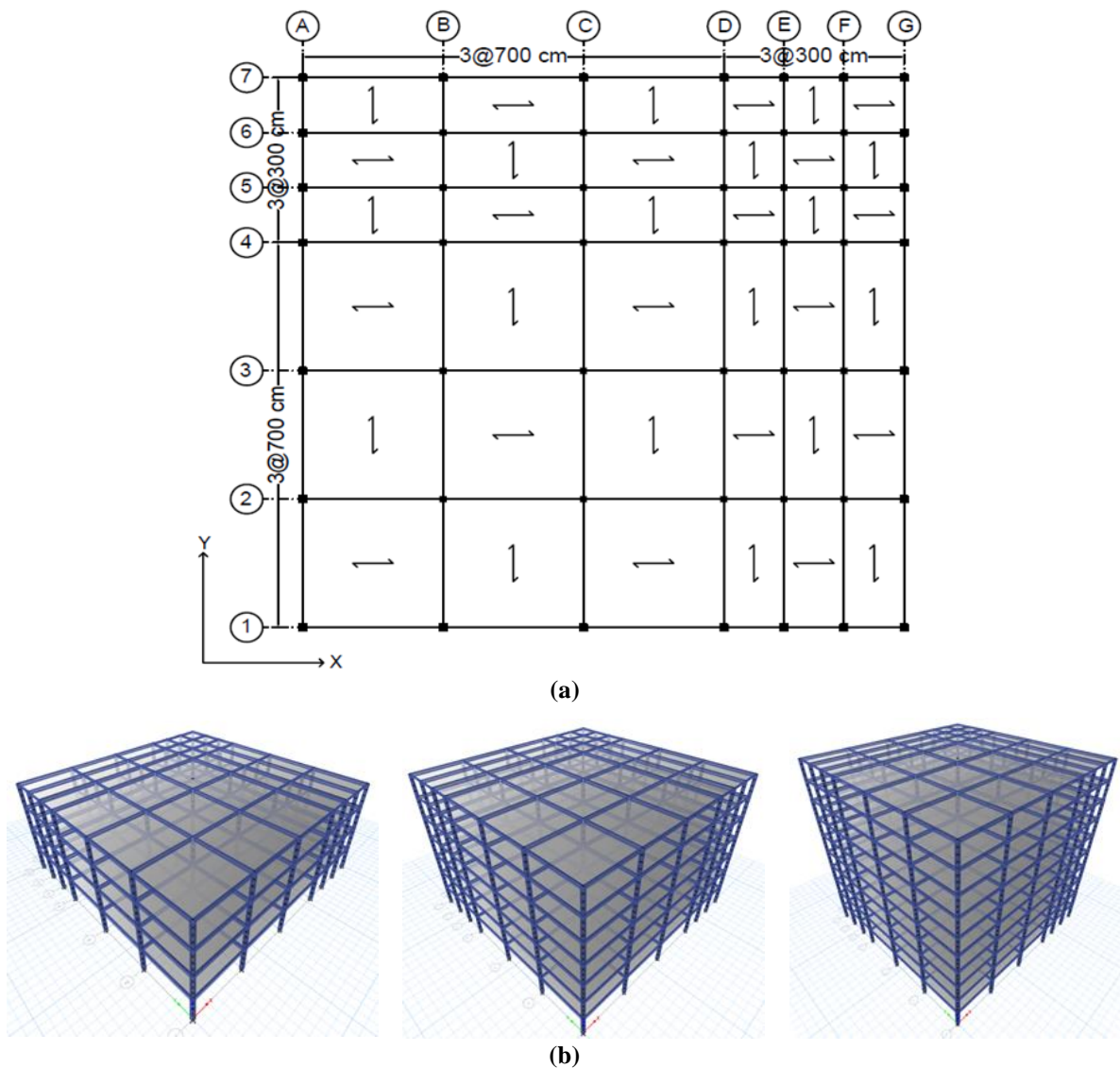
(a)

(b)

Fig. 4. The studied buildings: a) The common story plan; and b) The perspective

The structures shown in Figure 4 are in 4, 7, and 10 stories. They are composed of special steel moment frames with rigid diaphragms. The common story plan shows that the frame arrangement is irregular and the adjacent frame distances are smaller at the right and up sides of the plan. Then, if uniform frames are used, the center of stiffness will be at the North-East of the plan. In the design stage, the live load, similar to the dead load, is assumed to be uniformly distributed over the plans. However, at the stage of nonlinear dynamic analysis, the random nature of the live load will be considered by assuming different unsymmetric distribution of the same.

The common story height is 3.2 m. Values of the gravity loads are shown in Table 1.

Table 1. The gravity loads

Load type	Load intensity (KN/m²)
Floors dead load	5.5
Roof dead load	6.0
Floors live load	2.0
Roof live load	1.5
Partition load	1.0
Snow load	1.0

In addition to the values mentioned in Table 1, a line load of 7 kN/m is used at the location of the perimeter walls.

The site soil once is taken to be of the "C" type (stiff soil) and the other time is of the "D" type (firm soil) (ASCE/SEI 7-16, 2016). The buildings are located in a highly seismic area having the design spectra for the two soil types as shown in Figure 5 (ASCE/SEI 7-16, 2016).

Design of the structural frames is performed using AISC 360-16 (AISC360-16, 2016). The steel type used is St-37 having a yield strength of 240 MPa. At each story only two beam sections and four column sections are considered for keeping in line with practical considerations, as shown in Figure 6.

For the 4-story building, B1 beams appear to be IPE400 and B2 beams vary from IPE270 to IPE330. The C1-C4 columns are 320×25 to 340×25 boxes. In the 7-story building, the same members vary from IPE240 to IPE400 for the beams and from 260×20 to 340×25 boxes for the columns. For the 10-story building, the variation is from IPE240 to IPE400 for the beams and from 300×20 to 400×25 boxes for the columns. The fundamental periods of the designed buildings on the two soil types are mentioned in Table 2.
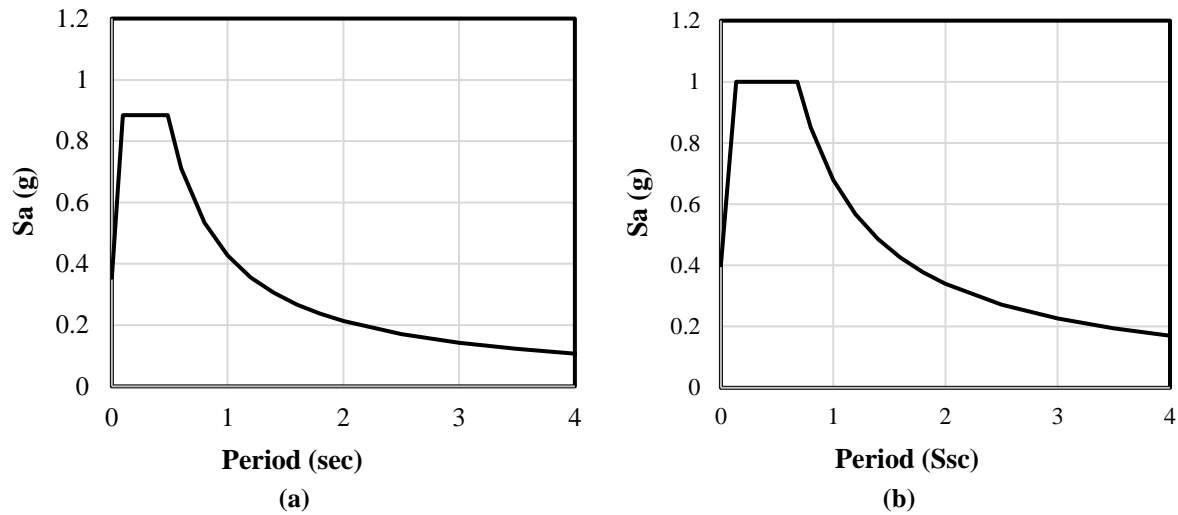

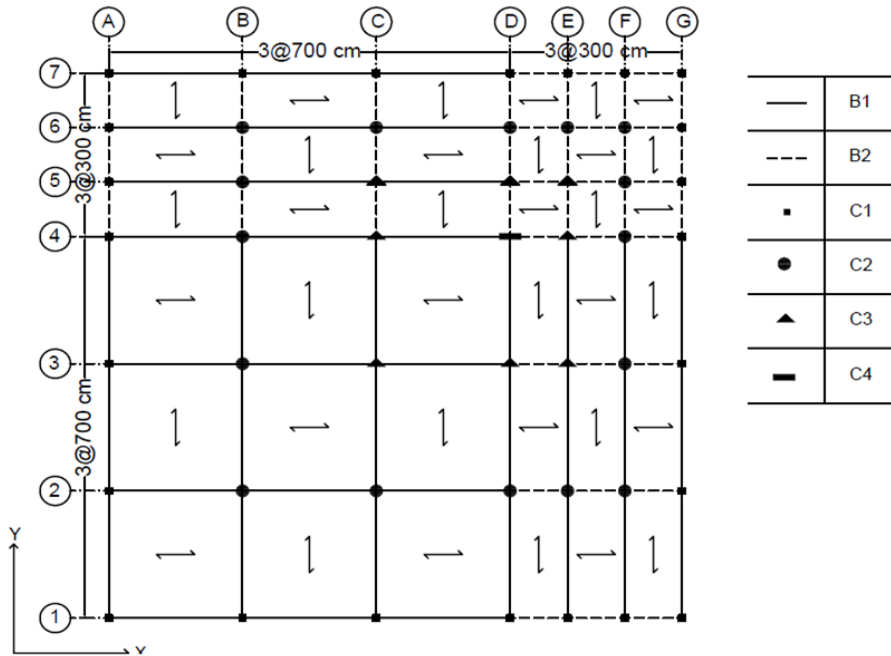**Fig. 5.** The design spectra: a) For the "C" type soil; and b) For the "D" type soil

Fig. 6. Beam and column types

Table 2. Fundamental periods of the buildings on each soil type.

No. of stories	Soil C	Soil D
4	0.839	0.741
7	1.480	1.269
10	2.073	1.763

4. Nonlinear Modelling of the Structures

The basic elements of a moment frame are its beams, columns, and panel zones. From the viewpoint of nonlinear modeling, the beams are different from the columns regarding the fact that they are mainly under a two-dimensional (2D) set of a single bending moment in addition to a vertical shear force. In contrast, the internal loads of a columns belong to a three-dimensional (3D) set of forces where in addition to the axial force, a pair of bi-directional bending moments act over the horizontal axes. Then, the nonlinear modelling of columns is much more complex than beams because the interaction between all three internal loads has to be taken into account. The third element, the panel zone, is a 2D medium under a set of 2D loads including an axial force, a bending moment, and horizontal and vertical shear forces acting over its four sides. Because of its small aspect ratio, its behavior is mainly governed by shear deformations.

Considering the above facts, the OpenSees software (McKenna, 2017) has been selected for this study. For modeling of line elements, i.e. beams and columns, it is possible to use the concepts of concentrated and/or distributed plasticity along the length of the members. Since the maximum bending moment under the combination of gravity and seismic loads generally happens only at the end points of the beams and columns, it is customary to assume that selecting a concentrated plasticity approach at such locations, while the rest of the members being free to act elastically, will suffice for engineering applications. The concentrated plasticity approach itself comes in two variations in OpenSees, including the completely-nonlinear moment-rotation (M-θ) spring and the bi-linear longitudinal fibers. The nonlinear M-θ spring has the advantage of modeling the post-elastic and stiffness/strength degradation of the member section. On the other hand, it cannot deal with bi-directional bending.

Therefore, it is suitable for modeling the nonlinear flexural behavior of beams only. The one-dimensional fiber elements are introduced by dividing the cross-section into several small areas and defining a fiber at each central point of the area elements along the member axis. Each fiber is known by its specific bi-linear stress-strain behavior. Altogether, the fibers comprise the whole cross section and its mechanical behavior. It is an ideal element for complex cross sections and loadings, but it can only result in a bi-linear behavior without stiffness/strength degradation. However, it is accurate enough if the flexural deformation, i.e. plastic hinge rotations, are not larger than small-enough values. Since in special moment frames the strong column-week beam rule applies, it is logical to anticipate that the inelastic action in the columns, if it happens ever in the frames under study, will not be much demanding. Therefore, the fiber elements are utilized for modelling the nonlinear behavior at the column ends. The fibers can be of steel01 or steel02 types; here the steel02 element is opted because of the more realistic gradual transition of stiffness between its two branches. The M-θ spring and the steel02 elements are shown in Figure 7.

For defining the steel02 material, the Young modulus and the yield strength of steel, E and F_y, respectively, and the post-yield elastic modulus reduction factors, b, have to be introduced. In fact, the b-factor shows the slope of the line connecting the yield point to the point of ultimate strength in the plane of stress-strain. Values of F_y, E, and b taken for St-37 steel in this study are 240 MPa, 206 GPa and 0.007, respectively.

The M-θ behavior shown in Figure 7 is defined by knowing M_y (yield moment), M_c (ultimate moment), c (residual moment factor), θ_y (yield rotation), θ_c (failure rotation), and θ_u (ultimate rotation), out of which, θ_c and θ_u are known by introducing the parameters a and b. This model is known as Bilin, or the modified Ibarra-Krawinkler model in OpenSees, and forms the basic backbone curve in ASCE 41-17

(2017). Its deterioration parameters are defined based on the works of Lignos and Krawinkler (2011). The relations and their numerical values for the above parameters based on the mentioned references as used in this study, are as follows.

The parameters *a*, *b*, and *c* in Figure 7, for the beams are functions of compactness of the section, shear characteristics and unbraced length. According to ASCE 41-17, for a beam with an I-shape and seismically compact section having sufficiently close lateral bracings, values of the mentioned parameters are a = $9\theta_y$, b = $11\theta_y$, and c = 0.6. The yield rotation θ_y, the shear effect factor η and the rate of cyclic deterioration Λ, can be calculated by Eqs. (1-3), respectively. Numerical values of the

parameters are mentioned in Table 3.

The rate of stiffness and strength cyclic deterioration is determined using the rule developed by Rahnama and Krawinkler (1993), which is defined on the basis of the hysteretic energy dissipated during the cyclic loading of the component. Each member is assumed to have a reference hysteretic energy dissipation capacity E_t, which is an intrinsic property of the components regardless of the applied loading history. The reference hysteretic energy dissipation capacity of the member is expressed as a multiple of Λ and M_y, where Λ and M_y are the reference cumulative rotation capacity and the effective yield strength of the component, respectively.

(a)

(b)
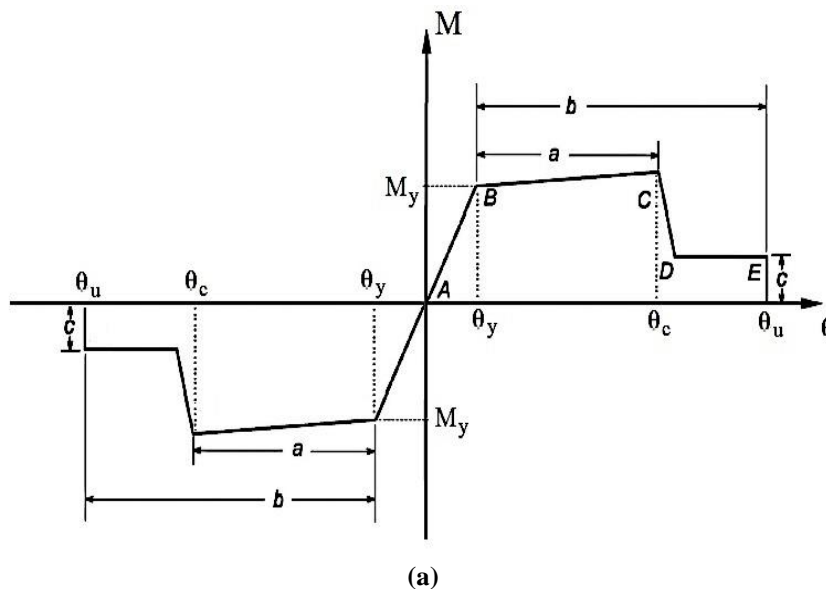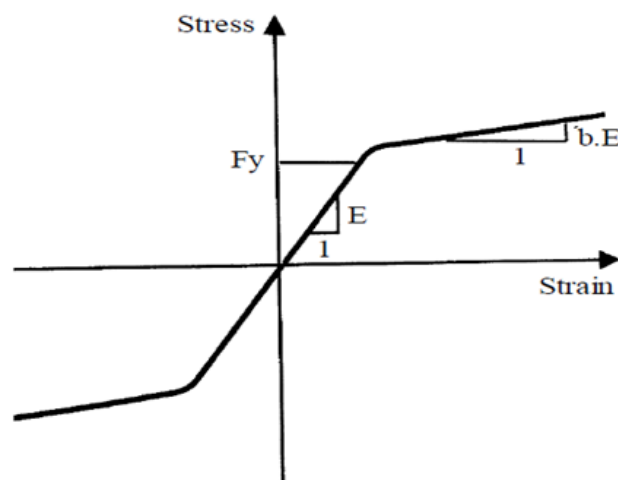
Fig. 7. a) The M-θ model for the beams per ASCE 41-17 (2017); and b) The steel02 material for the columns

Table 3. Nonlinear modeling parameters of the beams.

Beam section	Modeling parameters						
	a	b	c	θ_y	θ_c	θ_u	Λ
IPE240	0.041	0.050	0.600	0.005	0.046	0.055	1.631
IPE270	0.037	0.045	0.600	0.004	0.041	0.049	1.434
IPE300	0.033	0.041	0.600	0.004	0.037	0.044	1.319
IPE330	0.030	0.037	0.600	0.003	0.033	0.040	1.252
IPE360	0.028	0.034	0.600	0.003	0.031	0.037	1.244
IPE400 (spanning 3 m)	0.025	0.030	0.600	0.003	0.028	0.033	1.188
IPE400 (spanning 7 m)	0.058	0.071	0.600	0.006	0.064	0.077	1.188
IPE450	0.052	0.064	0.600	0.006	0.058	0.069	1.155

$$\theta_y = \frac{M_{pe}L(1+\eta)}{6EI} \tag{1}$$

$$\eta = \frac{12EI}{L^2 GA_s} \tag{2}$$

$$\Lambda = \frac{E_t}{M_y}$$
$$= 495(\frac{h}{t_w})^{-1.34}(\frac{b_f}{2t_f})^{-0.595}(\frac{c_{unit}^2 F_y}{355})^{-0.360} \tag{3}$$

Since the studied structures have been designed using contemporary building codes, it can be assumed that the panel zones will not suffer from bending or shear failure because of the use of appropriate continuity and (if needed) doubler plates. Then, it will be only necessary to take into account their flexibility as it can amplify the story drifts and consequently, add to the plastic hinge rotations. This effect can be dealt with either by continuing the beam line to the axis of columns in each span or by introducing a panel zone that includes elastic elements at the ends of beams through the column depth (Altoontash, 2004). In this study, the second approach has been selected to gain more accuracy. The elastic elements consist of a section including the continuity plates and the column web. Also, by assuming direct connection of the beam to the column, the distance from face of column to plastic hinge is considered to be zero.

5. The Ground Motions

The input records are used for IDA analysis. It means that first a set of appropriate earthquake records has to be selected for each building. Then, it should be scaled down and then gradually up, to be input to the model buildings to calculate their desirable responses at each scaled level of ground shaking. Therefore, at the first step the suitable ground motions have to be selected. The procedure recommended by ASCE 7-16 is followed for this purpose. Here it is meant to have a mean response spectrum of the selected earthquake records that does not fall below 90% of the design spectrum of Figure 5. The selection process is fulfilled in two steps. At the first step, all of the earthquake records that satisfy the criteria for three characteristics are chosen. The first step criteria are:

Magnitude between 6.5-7.5 (to be large enough), epicentral distance between 20-50 km (near-field effects are not meant), average shear wave velocity of the site soil being corresponding to the soil type C (366-762 m/sec) or D (183-365 m/sec) per case.

Following the above procedure, 131 and 193 pairs of earthquake records are found for the soil types C and D, respectively, using the PEER NGA database.

ASCE 7-16 requires that number of earthquake record pairs to be at least 11 for the nonlinear dynamic analysis of each building. It also recommends use of the records of only one station for each earthquake to prevent the analysis from being biased toward that seismic motion. Then, since number of the selected earthquakes is more than 11 for each soil type, and there are multiples of stations for a certain earthquake, the second step is taken by calculating the Square Root of Sum of the Squares (SRSS) of the pair of

response spectra of each ground motion. For each SRSS spectrum, a scale factor is calculated such that nowhere between 0.2T-2T, it falls below 90% of the corresponding design spectrum of Figure 5, where T: is the fundamental period of the building under study. It means that after scaling, at the lowest point each SRSS spectrum will only touch the 90% design spectrum. Between different stations of a specific earthquake, the one having the nearest scale factor to unity is selected. Again, between different earthquakes, the first 11 ground motions with their selected SRSS spectra having scale factors closer to unity are chosen. This way, the records with maximum similarity to the seismic nature, i.e. design spectrum, of the site are selected for analysis.

The earthquakes records selected for each building as a result of the above procedure are listed in Table 4. The SRSS response spectra of the selected records are shown in Figure 8.

Table 4. The selected earthquake records: a) For the C type soil; and b) For the D type soil

| Order	NGA No.	Earthquake name	Year	Magnitude	PGA (g)	For buildings having No. of stories equal to:
(a)						
1	15	Kern County	1952	7.36	0.180	4, 7, 10
2	78	San Fernando	1971	6.61	0.151	10
3	79	San Fernando	1971	6.61	0.109	4, 7
4	755	Loma Prieta	1989	6.93	0.485	4
5	787	Loma Prieta	1989	6.93	0.277	7, 10
6	963	Northridge-01	1994	6.69	0.568	4, 7, 10
7	1762	Hector Mine	1999	7.13	0.182	4, 7, 10
8	3750	Cape Mendocino	1992	7.01	0.265	4, 7, 10
9	3756	Landers	1992	7.28	0.188	4, 7
10	3757	Landers	1992	7.28	0.139	10
11	4016	San Simeon_ CA	2003	6.52	0.165	4, 7, 10
12	4213	Nigata	2004	6.63	0.405	4, 7, 10
13	4858	Chuetsu-Oki_ Japan	2007	6.80	0.251	4, 10
14	4868	Chuetsu-Oki_ Japan	2007	6.80	0.180	7
15	6891	Darfield_ New Zealand	2010	7.00	0.109	7
16	6948	Darfield_ New Zealand	2010	7.00	0.146	4
17	6971	Darfield_ New Zealand	2010	7.00	0.116	10
(b)						
1	20	Northern Calif-03	1954	6.50	0.203	4, 7, 10
2	169	Imperial Valley-06	1979	6.53	0.350	4, 7, 10
3	730	Spitak_ Armenia	1988	6.77	0.200	4, 7, 10
4	776	Loma Prieta	1989	6.93	0.370	4, 7, 10
5	958	Northridge-01	1994	6.69	0.125	4, 7, 10
6	1100	Kobe_ Japan	1995	6.90	0.231	4
7	1110	Kobe_ Japan	1995	6.90	0.210	7, 10
8	3754	Landers	1992	7.28	0.310	7, 10
9	3758	Landers	1992	7.28	0.116	4
10	4849	Chuetsu-Oki_ Japan	2007	6.80	0.250	10
11	4853	Chuetsu-Oki_ Japan	2007	6.80	0.274	4, 7
12	5780	Iwate_ Japan	2008	6.90	0.354	4
13	5814	Iwate_ Japan	2008	6.90	0.320	7, 10
14	5988	El Mayor-Cucapah_ Mexico	2010	7.20	0.280	7, 10
15	5990	El Mayor-Cucapah_ Mexico	2010	7.20	0.255	4
16	6923	Darfield_ New Zealand	2010	7.00	0.360	7, 10
17	6953	Darfield_ New Zealand	2010	7.00	0.220	4

(a)

(b)
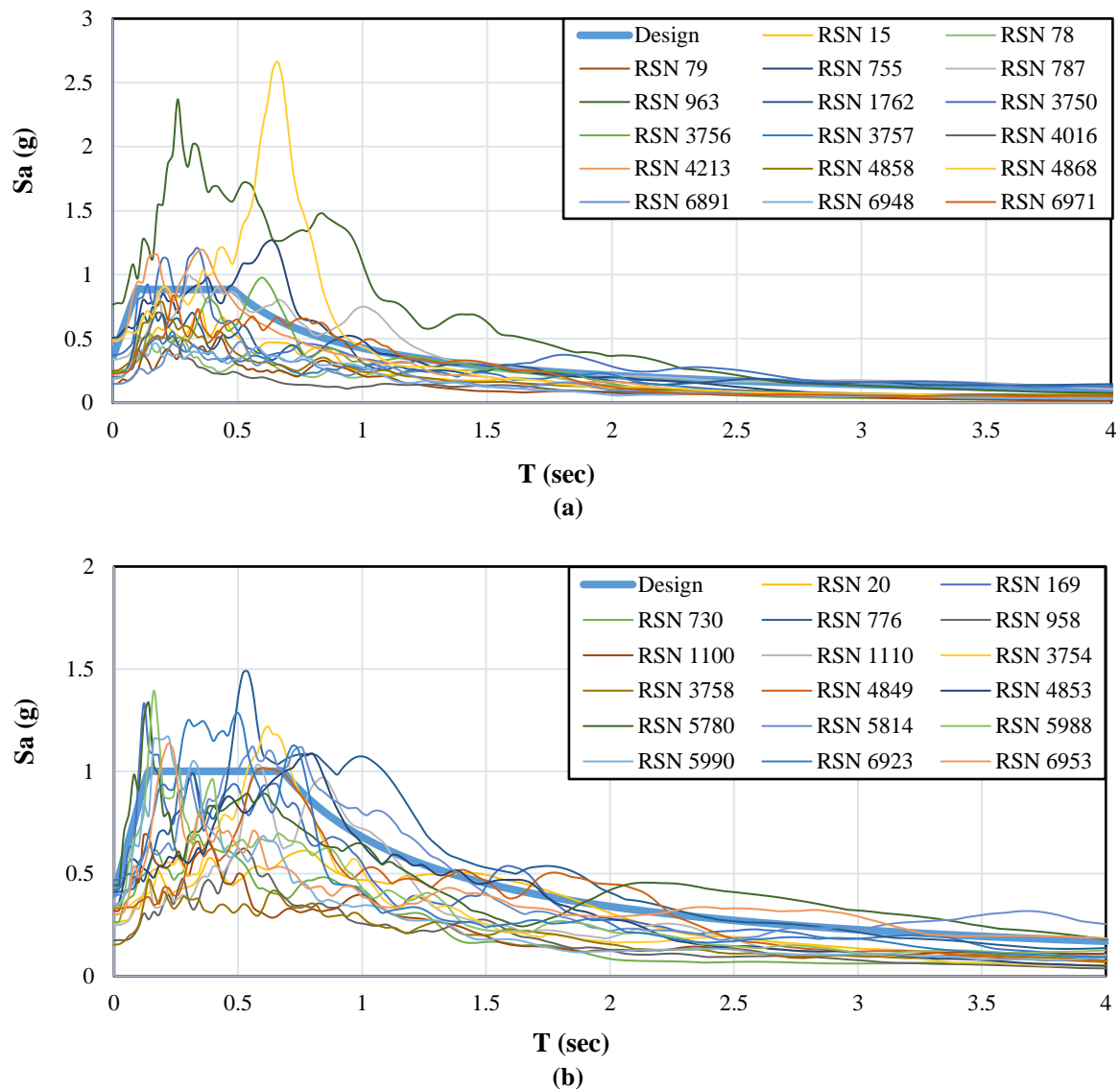
Fig. 8. The SRSS response spectra of the selected records: a) For the "C" type soil; and b) For the "D" type soil

6. Results of the Analysis

The nonlinear dynamic analysis results are presented in this section. In the first part, a verification study is accomplished. Then, the various cases of torsional eccentricity are introduced. Finally, nonlinear dynamic responses are presented.

6.1. The Verification Study

To assess the accuracy of the nonlinear modeling as described in Section 4, the 4-story building of Farahani et al. (2019) is selected. The configuration of that building is very similar to the 4-story structure of the current study. In Figure 8, time history of the lateral displacement of the roof is shown under the Loma Prieta earthquake, NGA

No. 755. A very good similarity of responses between the original and current study is observed. The maximum relative differences between the responses is only about 10%.

6.2. Torsional Eccentricity Cases

According to the common plan of the buildings (Figure 4), center of stiffness is deviated toward North-East. Also, as explained in Section 2, assuming eccentricity ratios larger than 10-15% is not realistic for moment frame buildings. Then, the study is implemented for the eccentricity ratios 0%, 5%, 10%, and 15%. To make for such eccentricities, the plan is divided into some subdomains and a certain part of the total partition and live loads is

applied on each area such that the presumed torsional eccentricity is attained. It is to be noted that the total value of the partition plus live loads is the same in all of the cases. It is equal to the total load mentioned in

Section 3.

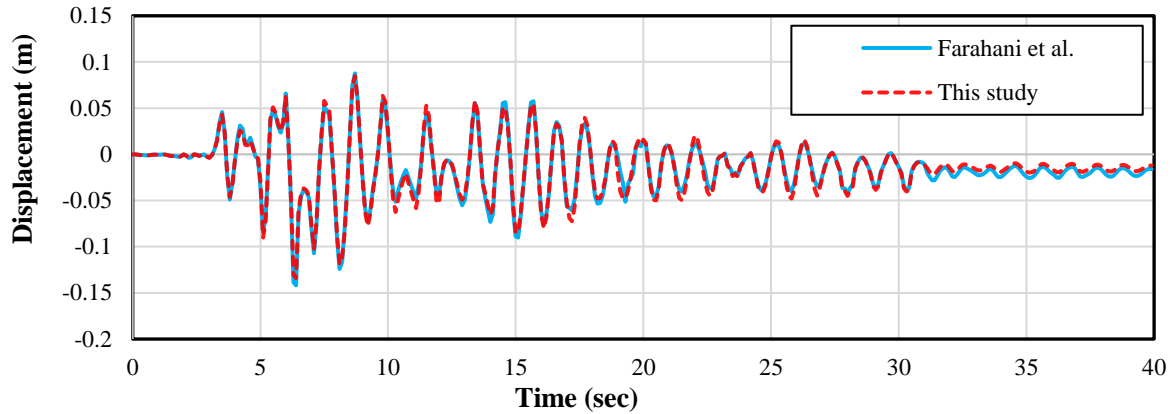The plan configuration and each superimposed load in each area are shown in Figure 9.

Fig. 9. Time history of the roof displacement of the 4-story building of Farahani and Behnamfar (2019)
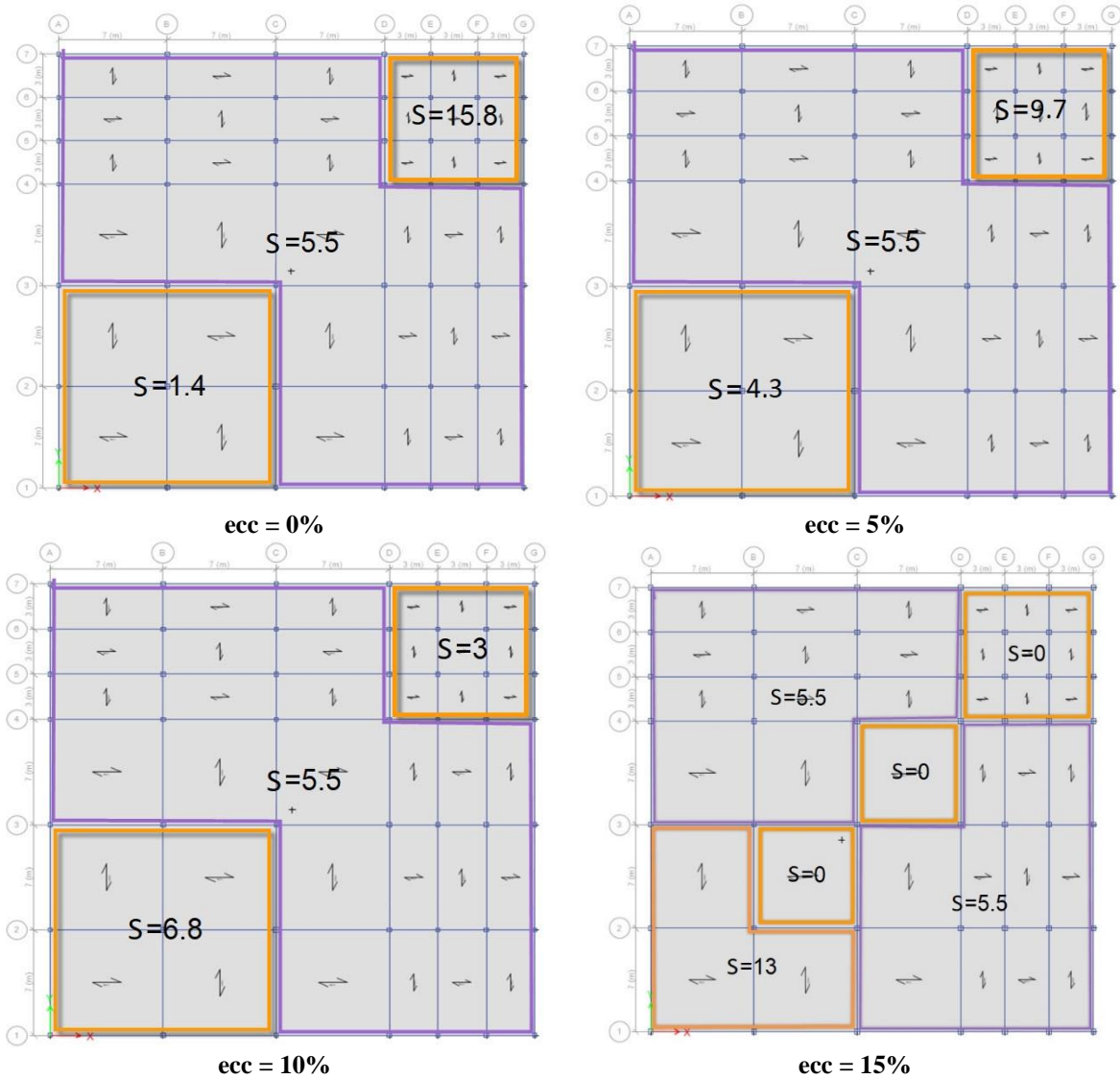

Fig. 10. Value of the superimposed loads in each part of the plan and the corresponding torsional eccentricity (ecc). S is for superimposed and each number is the load intensity in KN/m^2

It is to be reminded that the buildings were designed for a uniform superimposed load. It is assumed that change in the load distribution happens afterwards during service.

6.3. The Analysis Results

The IDA and fragility curves have been calculated for the 4, 7, and 10-story buildings having four cases of torsional eccentricity on two types of soils. Therefore, presenting all of the calculated results is not possible. Instead, it is opted to present details of the computation for the 4-story building on the soil type C for example, and then the final results for other buildings and for the soil type D.

6.3.1. Analysis Results of the 4-Story Building on the Soil Type C

The IDA curves of the 4-story building are illustrated in Figure 10. In this figure, each seismic record is amplified in sequences almost 20 times to finally make the building to reach its collapse state, where the lateral stiffness is almost zero. At each intensity level for each earthquake, the maximum interstory drift is determined for the building and marked as a point on the IDA plot against the first-mode spectral acceleration of the same building at the same shaking level. The IDA curve if drawn by connecting these points together. It should be noted that the maximum drift happens at a certain story on the soft side of the plan.
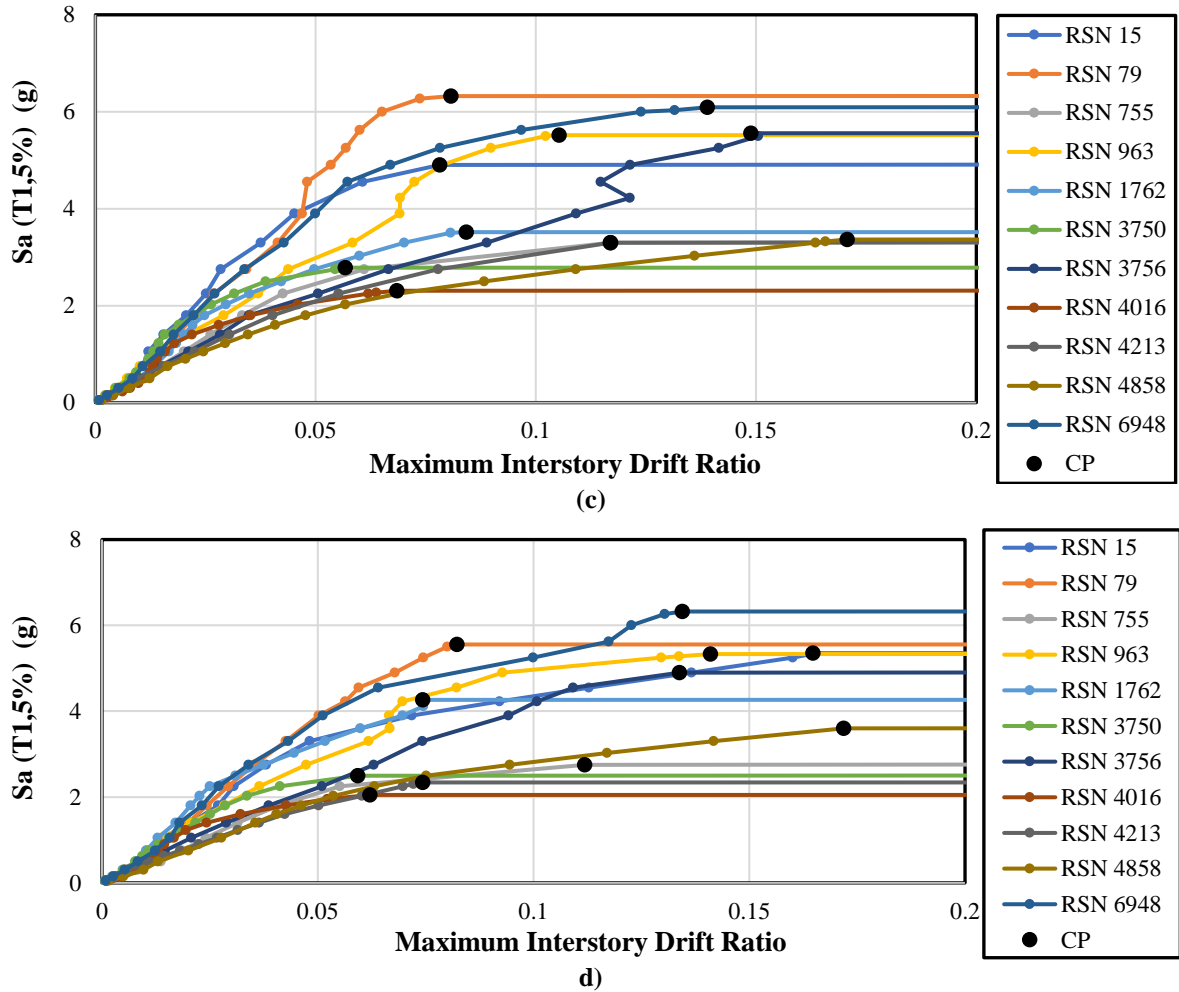

(a)

(b)
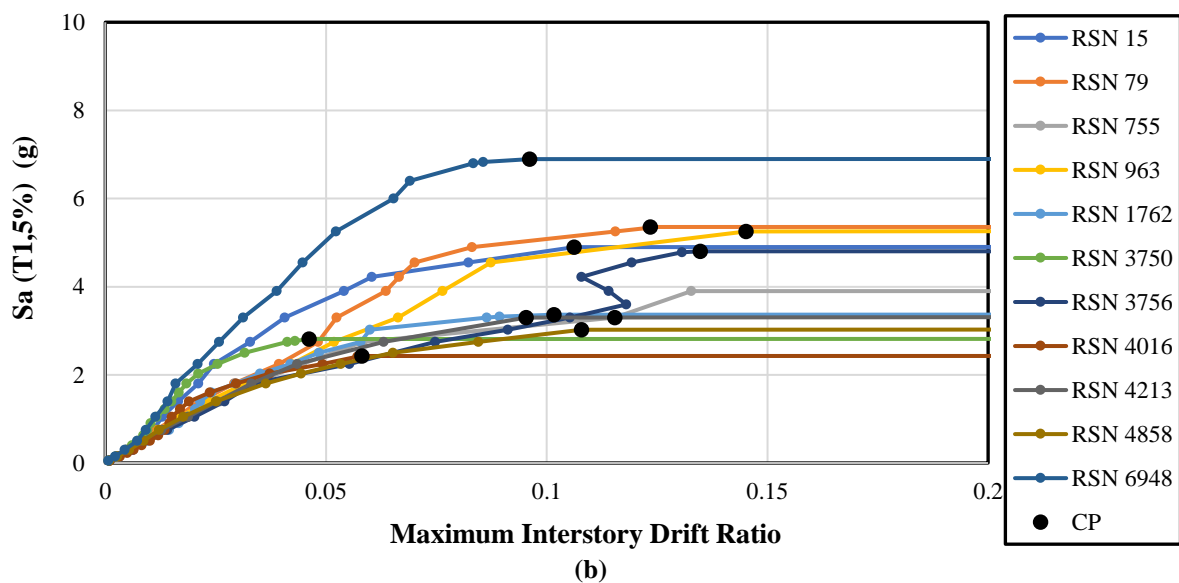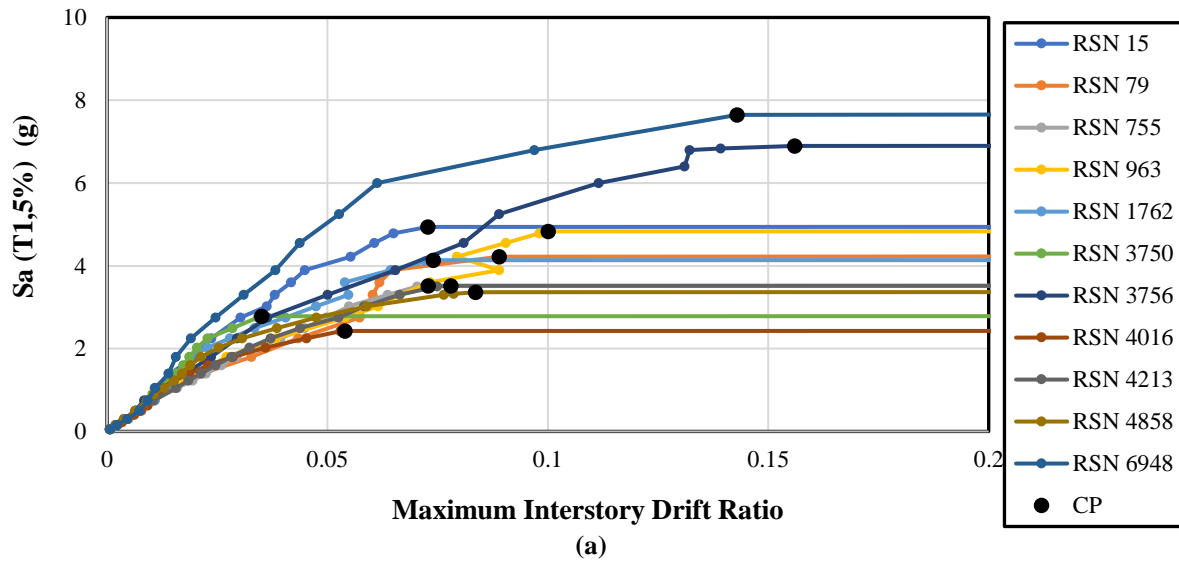
Fig. 11. The IDA curves of the 4-story building on the soil type C for the eccentricity ratios of: a) 0%; b) 5%; c) 10%; and d) 15%

Each of the four parts of Figure 10 gives 11 values of collapse spectral acceleration. If a Log-Normal distribution is assumed for these 11 values, it will be possible to depict the fragility curve that represents the probability of collapse against the increasing spectral accelerations. The resulting curves are shown for various eccentricities in the case of the 4-story building on the soil types C and D in Figure 11.

Similarly, fragility curves of the other buildings on both soil types are shown in Figures 13 and 14.
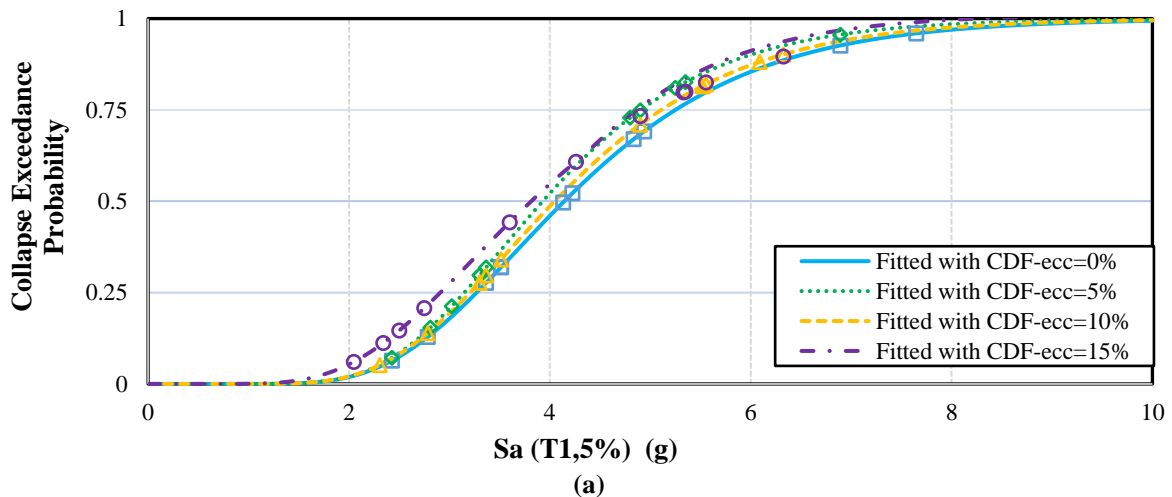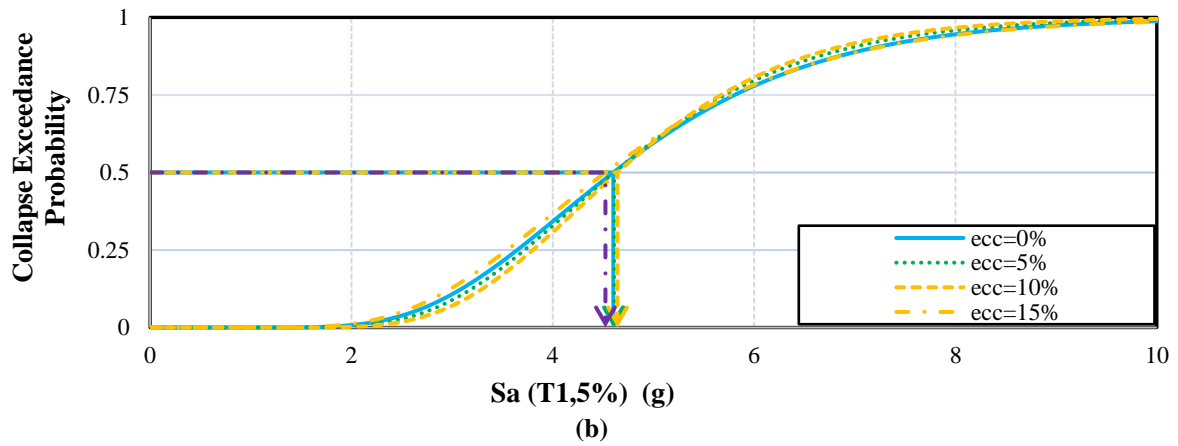
Fig. 12. Fragility curves of the 4-story building under various eccentricities on the soil types: a) C; and b) D
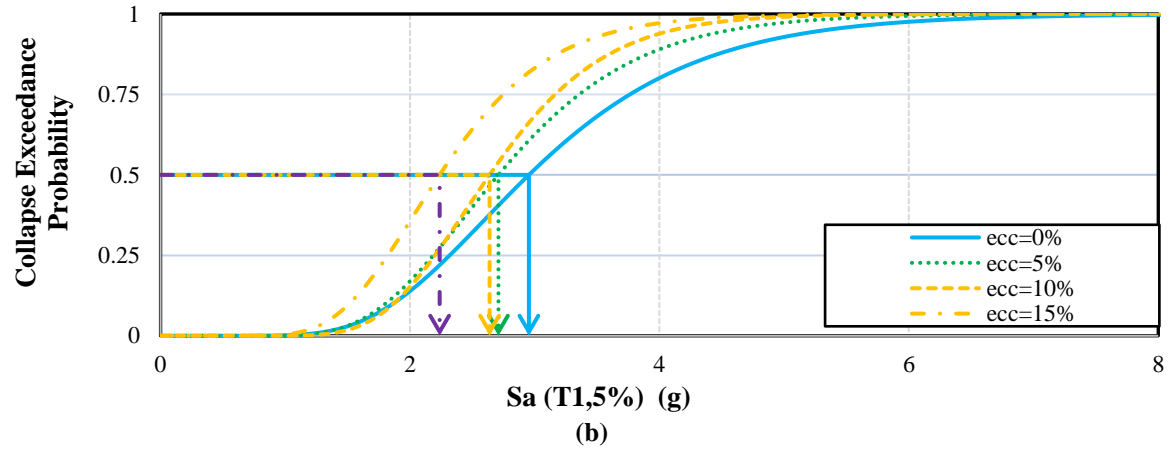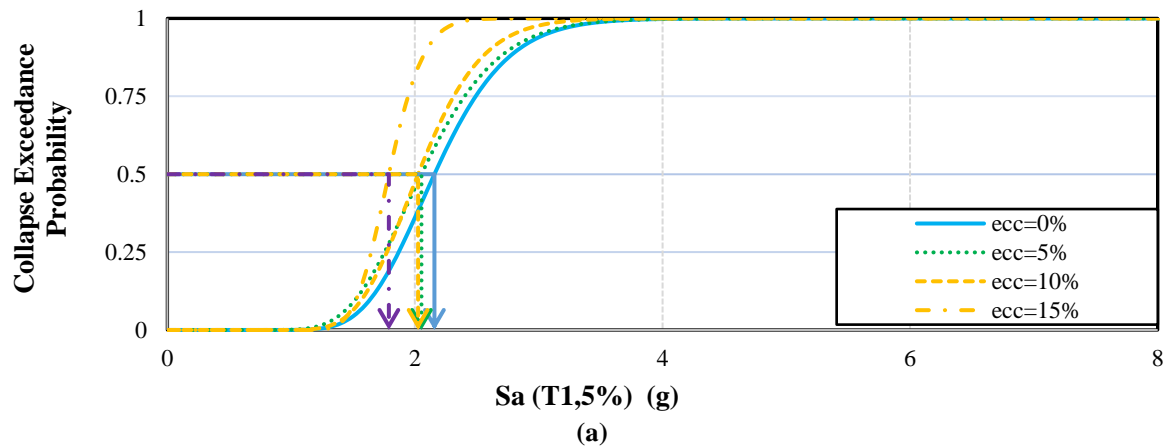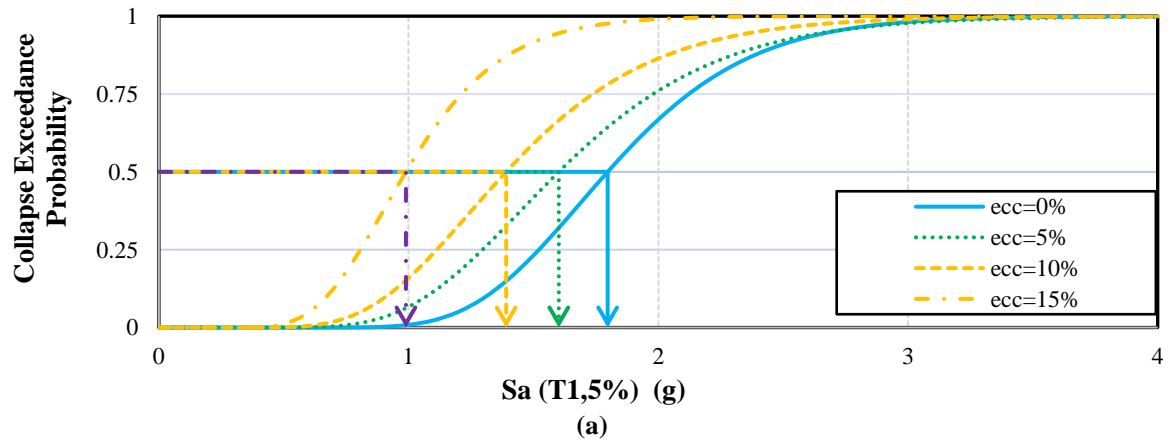

Fig. 13. Fragility curves of the 7-story building on the soil types: a) C; and b) D
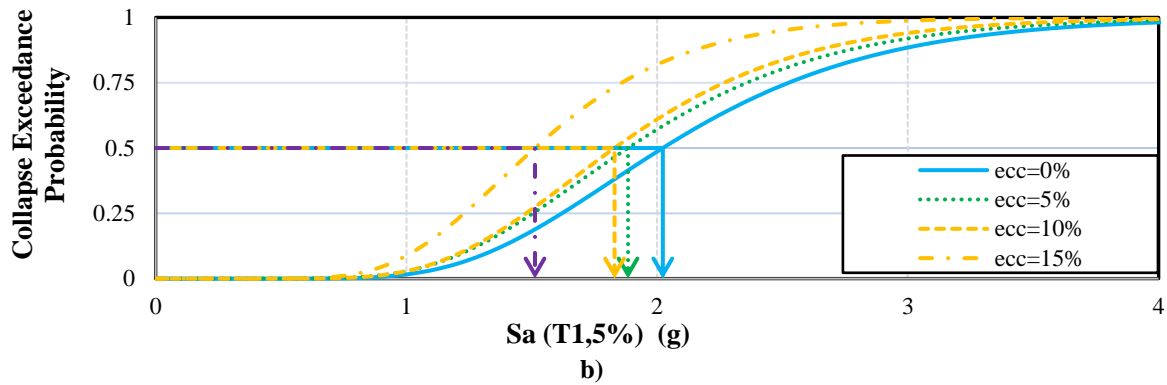
Fig. 14. Fragility curves of the 10-story building on the soil types: a) C; and b) D

As demonstrated in the above figures, in general, increase of torsional eccentricity results in decrease of the collapse spectral acceleration for a certain probability, or in increase of the collapse probability for a certain spectral acceleration.

To have some numerical criteria for comparison, the spectral acceleration at the mean (50%) collapse probability is selected. Furthermore, the Collapse Margin Ratio (CMR) is calculated for each case. It is defined as follows:

$$CMR = \frac{S_{CT}}{S_{MT}} \times C_{3D} \qquad (4)$$

where S_{CT} and S_{MT}: are the median collapse and the maximum considered earthquake (MCE) spectral accelerations at the fundamental period of the building, respectively, and C_{3D}: is a correction coefficient equal to 1.0 for 2D and 1.2 for 3D analysis to account for the effect of simultaneous ground motion pairs in the latter analysis. Values of the above parameters are summarized in Table 5 for the soil type C and in Table 6 for the soil type D.

Moreover, Tables 7 and 8 exhibit the reduction percentages of CMR relative to the no-torsion (i.e. zero eccentricity) cases.

Table 5. Collapse margin ratio for the buildings on the soil type C: a) 4-story; b) 7-story; and c) 10-story building

No. of stories	S_a (g)	S_{MT} (g)	S_{CT} (g)				CMR			
			e=0%	e=5%	e=10%	e=15%	e=0%	e=5%	e=10%	e=15%
4	0.77	1.15	4.16	3.95	4.05	3.80	4.34	4.23	4.12	3.97
7	0.49	0.74	2.16	2.05	2.02	1.78	3.53	3.35	3.30	2.91
10	0.37	0.56	1.80	1.60	1.39	0.98	3.89	3.46	3.01	2.12

Table 6. Collapse margin ratio for the buildings on the soil type D: a) 4-story; b) 7-story; and c) 10-story building

No. of stories	S_a (g)	S_{MT} (g)	S_{CT} (g)				CMR			
			e=0%	e=5%	e=10%	e=15%	e=0%	e=5%	e=10%	e=15%
4	0.92	1.38	4.58	4.57	4.64	4.52	3.99	3.98	4.04	3.94
7	0.78	1.17	2.95	2.71	2.63	2.25	3.02	2.78	2.69	2.30
10	0.59	0.88	2.03	1.90	1.82	1.52	2.77	2.59	2.48	2.07

Table 7. Reduction percentages of CMR relative to the no-torsion cases, soil type C.

No. of stories	ecc=5%	ecc=10%	ecc=15%
4	2.6%	5.1%	8.7%
7	5.1%	6.5%	17.6%
10	11.1%	22.8%	45.6%

Table 8. Reduction percentages of CMR relative to the no-torsion cases, soil type D

No. of stories	ecc=5%	ecc=10%	ecc=15%
4	0.2%	1.3%	1.3%
7	8.1%	10.9%	23.7%
10	6.4%	10.3%	25.1%

The above tables clearly show how increase of the torsional eccentricity reduces the collapse margin ratio hence the safety of the buildings. Notably, the decrease of CMR is much more extensive when the eccentricity ratio increases from 10 to 15%. Note that the more significant effect of torsion seen for taller structures is somewhat exaggerated because possibility of existence of a uniform simultaneous eccentricity at all stories, assumed in this study, is low.

Moreover, the reduction percentages are different for the buildings on the two soil types. The design spectral ordinates are larger for the softer soil. The buildings designed under the design spectrum belonging to this soil type are more or less, stronger than their counterparts on the soil type C. Of course, the input motion is correspondingly larger too. Since the ground motions are different for the two soil type cases, finding a ready reason is not possible for the observed difference between the CMR values for similar cases on the two soil types.

For the taller buildings of this study, the CMR reduction surpasses a desirable 10% threshold sooner, i.e. under smaller eccentricities. Therefore, the design regulations of buildings should be modified in such a way that results in more or less identical CMRs for different buildings at similar eccentricities.

In the following, results of the present study are compared with two similar studies.

In the study of Manie et al (2015), described in the Introduction, the collapse behavior of asymmetric RC-SMF structures was evaluated. The studied buildings were in three and six stories with one-way mass eccentricity and were subjected to two-component earthquakes. According to the IDA curves in terms of SRSS drift of the 6-story structures, reduction percentage of the safety margin compared to structures without torsion were respectively 0%, 37% and 42% for structures with eccentricity ratios of 10%, 20% and 30%. Thus, for structures with eccentricity ratios of more than 10%, reduction of the safety margin was considerable. Therefore, it can be said that the results of the mentioned study are in good agreement with those of the seven- and ten-story structures of the present study, where the case of 15% eccentricity ratio significantly affects the safety margin.

Badri et al. (2016) investigated effects of variability of deterioration parameters on the response of RC-SMF buildings. The studied five-story buildings assumed to be either symmetrical or having 10% or 20% mass eccentricity under unidirectional earthquakes. Comparison of the IDA curves of the studied structures showed that increasing the eccentricity of the structures had a slight decreasing effect on the collapse spectral acceleration. Therefore, the results of their study are consistent with the results of the four-story structure of the present study.

Finally, by reviewing the previous studies, it can be said that only a small number of studies include explicit results related to the effect of torsion on the structure collapse behavior. Also, the range of their studied structures are limited. The results of these few studies are not completely consistent with each other, which may be due to their different assumptions. One of the advantages of the present study is the wider range of structures studied here than the previous studies, which can lead to more comprehensive and reliable conclusions.

7. Conclusions

Fragility curves of 4, 7 and 10-story special steel moment frames were calculated each one under 11 consistent pairs of earthquake motions on two types of soils in this study. The torsional irregularity of the buildings was the result of bi-directional simultaneous stiffness and mass eccentricities. It was observed that:
- Based on a discussion conducted in the form of examples with exaggerated eccentricity conditions, after the final

design process of moment frame systems, the stiffness center was shifted and the torsional eccentricity was reduced considerably. Therefore, it seems that assuming large eccentricity values for moment frame structures in previous studies has not been realistic.

- With regard to the previous item, it can be said that taking eccentricity ratios more than about 15% is not realistic for moment frame buildings. The current building design regulations tend to decrease the eccentricity in final design of the members.

- The median collapse probabilities of the studied buildings were increased by torsional eccentricity. Value of the increase was not considerable up to an eccentricity ratio equal to about 10%. Eccentricity ratios larger than 10% had a significant effect on the collapse behavior of 7 and 10-story buildings.

- For the eccentricity ratio of 15%, the amount by which the collapse margin ratio decreased was extensive, especially for the taller buildings. Such eccentricities should be prevented in real design tasks. Accordingly, seismic building code should be more developed and specific to eccentricity ratios larger than 10%.

- Effect of torsion on the collapse margin ratio of the studied buildings designed for stiffer soil conditions was generally more extensive, even though their base was assumed to be fixed. Further studies on the structural torsion on different soils should account for base flexibility.

As a final point of consideration, it should be mentioned that the main limitations of this study are the facts that it includes short and midrise buildings (up to 10 stories) consisting of special steel moment frames on two types of soils (stiff and firm).

Though the results are specifically applicable to the cases within the same limitations, conclusions that can be named to be the generally applicable findings of this study are as follows.

Regarding the realistic limit of the eccentricity ratio, the fact that torsional eccentricity increases the collapse probability especially for taller buildings and the effect of soil flexibility on the collapse probability due to torsional eccentricity requires more research.

8. References

AISC360-16. (2016). *Specification for structural steel buildings*, American Institute of Steel Construction (AISC), Chicago.

Altoontash, A. (2004). "Simulation and damage models for performance assessment of reinforced concrete beam-column joints", Ph.D. Thesis, Stanford University Stanford, California.

Anvarsamarin, A., Rahimzadeh Rofooei, F. and Nekooei, M. (2020). "Torsion effect on the RC structures using fragility curves considering with soil-Structure interaction", *Journal of Rehabilitation in Civil Engineering*, 8(1), 1-21. https://doi.org/10.22075/jrce.2019.16080.1302.

ASCE/SEI 7-16. (2016). *Minimum design loads and associated criteria for buildings and other structures*, ASCE Standard ASCE/SEI 7-16, American Society of Civil Engineers (ASCE).

ASCE41-17. (2017). *Seismic rehabilitation of existing buildings,* ASCE Standard ASCE/SEI 41-17, American Society of Civil Engineers (ASCE).

Ashwini, P. and Stephen, S. (2022). "Seismic fragility analysis of structures containing supplemental damping system", *International Journal of Scientific and Research Publications*, 12(1), 417-425, https://doi.org/10.29322/IJSRP.12.01.2022.p12 156.

Aziminejad, A. and Moghadam, A. (2010). "Fragility-based performance evaluation of asymmetric single-story buildings in near field and far field earthquakes", *Journal of Earthquake Engineering,* 14(6), 789-816, https://doi.org/10.1080/13632460902837728.

Badri, R.K., Moghadam, A. and Nekooei, M. (2016). "The influence of deterioration parameters on the response of low-rise symmetric and asymmetric RC buildings", *International Journal of Civil Engineering,* 14(8), 547-560, https://doi.org/10.1007/s40999-016-0038-x.

Bensalah, M.D., Bensaibi, M. and Modaressi, A. (2013). "Assessment of the torsion effect in asymmetric buildings under seismic loading", *Applied Mechanics and Materials*, 256, 2222-2228, https://doi.org/10.4028/www.scientific.net/AM M.256-259.2222.

Chen, P. and Collins, K.R. (2001). "Some observations on performance-based and

reliability-based seismic design of asymmetric building structures", *Engineering Structures,* 23(8), 1005-1010, https://doi.org/10.1016/S0141-0296(00)00108-5.

Chiou, B., Darragh, R., Gregor, N. and Silva, W. (2008). "NGA project strong-motion database", *Earthquake Spectra*, 24(1), 23-44, https://doi.org/10.1193/1.2894831.

Collins, K., Wen, Y.K. and Foutch, D. (1996). "Dual-level seismic design: a reliability-based methodology", *Earthquake Engineering & Structural Dynamics,* 25(12), 1433-1467, https://doi.org/10.1002/(SICI)1096-9845 (199612)25:12<1433::AID-EQE629>3.0.CO;2-M.

Das, P.K., Dutta, S.C. and Datta, T.K. (2021). "Seismic behavior of plan and vertically irregular structures: State of art and future challenges", *Natural Hazards Review*, 22(2), 04020062, https://doi.org/10.1061/(ASCE)NH.1527-6996.0000440.

DeBock, D.J., Liel, A.B., Haselton, C.B., Hooper, J.D. and Henige, R.A. Jr. (2014). "Importance of seismic design accidental torsion requirements for building collapse capacity", *Earthquake Engineering & Structural Dynamics,* 43(6), 831-850, https://doi.org/10.1002/eqe.2375.

Dehghani, E. and Soltanimohajer, M. (2022). "Development of the fragility curves for conventional reinforced concrete moment resistant frame structures in Qods Town, Qom City, Iran", *Civil Engineering Infrastructures Journal*, 55(1), 31-41, https://doi.org/10.22059/CEIJ.2021.306156.1690.

De Stefano, M. and Pintucchi, B. (2008). "A review of research on seismic behaviour of irregular building structures since 2002", *Bulletin of Earthquake Engineering*, 6(2), 285-308, https://doi.org/10.1007/s10518-007-9052-3.

De Stefano, M. and Mariani, V. (2014). "Pushover analysis for plan irregular building structures", *Perspectives on European Earthquake Engineering and Seismology,* 34, 429-448, https://doi.org/10.1007/978-3-319-07118-3_13.

Eivani, H., Moghadam, A.S., Aziminejad, A. and Nekooei, M. (2018). "Seismic response of plan-asymmetric structures with diaphragm flexibility", *Shock and Vibration*, 2018, 1-18, https://doi.org/10.1155/2018/4149212

Elghazouli, Y. (2010). "Assessment of European seismic design procedures for steel framed structures", *Bulletin of Earthquake Engineering*, 8, 65-89, http://doi.org/10.1007/s10518-009-9125-6.

Farahani, D., Behnamfar, F., Sayyadpour, H. and Ghandil, M. (2019). "Seismic impact between adjacent torsionally coupled buildings", *Soil Dynamics and Earthquake Engineering,* 117, 81-

95, https://doi.org/10.1016/j.soildyn.2018.11.015.

Fujii, K. (2014). "Prediction of the largest peak nonlinear seismic response of asymmetric buildings under bi-directional excitation using pushover analyses", *Bulletin of Earthquake Engineering,* 12(2), 909-938, http://doi.org/10.1007/s10518-013-9557-x.

Ferraioli, M., Lavino, A., Mandara, A. (2014). "Behaviour factor of code-designed steel moment-resisting frames", *International Journal of Steel Structures*, 14(2), 243-254, http://doi.org/10.1007/s13296-014-2005-1.

Ferraioli, M. (2015). "Case study of seismic performance assessment of irregular RC buildings: hospital structure of Avezzano (L'Aquila, Italy)", *Earthquake Engineering and Engineering Vibration*, 14(1), 141-156, http://doi.org/10.1007/s11803-015-0012-7.

Gioncu, V. and Mazzolani, F. (2010). *Seismic design of steel structures*, Taylor & Francis Ltd., https://doi.org/10.1201/b16053.

Habiby, Y.M. (2020). "Collapse analysis of torsional moment frame structures against earthquake", M.Sc. Thesis, Isfahan University of Technology. Han, S.W., O Kim, T., Kim, D.H. and Baek, S.J. (2017). "Seismic collapse performance of special moment steel frames with torsional irregularities", *Engineering Structures,* 141, 482-494, https://doi.org/10.1016/j.engstruct.2017.03.045.

Hentri, M., Hemsas, M. and Nedjar, D. (2018). "Vulnerability of asymmetric multi-storey buildings in the context of performance-based seismic design", *European Journal of Environmental and Civil Engineering,* 25, 1-22, http://doi.org/10.1080/19648189.2018.1548380.

Hwang, S.-H., Mangalathu, S., Shin, J., and Jeon, J.-S. (2021). "Machine learning-based approaches for seismic demand and collapse of ductile reinforced concrete building frames", *Journal of Building Engineering*, 34, 101905, https://doi.org/10.1016/j.jobe.2020.101905.

Kazemi, F. and Jankowski, R. (2023). "Machine learning-based prediction of seismic limit-state capacity of steel moment-resisting frames considering soil-structure interaction", *Computers & Structures*, 274, 106886, https://doi.org/10.1016/j.compstruc.2022.106886.

Landolfo, R. (2018). "Seismic design of steel structures: New trends of research and updates of Eurocode 8", *Geotechnical, Geological and Earthquake Engineering,* 46, 413-438, http://doi.org/10.1007/978-3-319-75741-4_18.

Lignos, D.G. and Krawinkler, H. (2011). "Deterioration modeling of steel components in support of collapse prediction of steel moment frames under earthquake loading", *Journal of Structural Engineering,* 137(11), 1291-1302,

http://doi.org/10.1061/(ASCE)ST.1943-541X.0000376.

Manie, S., Moghadam, A.S. and Ghafory-Ashtiany, M. (2015). "Collapse behavior evaluation of asymmetric buildings subjected to bi-directional ground motion", *The Structural Design of Tall and Special Buildings,* 24(8), 607-628, https://doi.org/10.1002/tal.1202.

Marušić, D. and Fajfar, P. (2005). "On the inelastic seismic response of asymmetric buildings under bi-axial excitation", *Earthquake Engineering & Structural Dynamics,* 34(8), 943-963, https://doi.org/10.1002/eqe.463.

Mazzolani F.M. and Piluso V. (1996). *Theory and design of seismic resistant steel frames*, E & FN SPON, an imprint of Chapman & Hall, London, https://doi.org/10.1201/9781482271348.

McKenna, F. (2011). "OpenSees: A framework for earthquake engineering simulation", *Computing in Science & Engineering,* 13(4), 58-66, https://doi.org/10.1109/MCSE.2011.66.

Moon, D.S., Lee, Y.J. and Lee, S. (2018). "Fragility analysis of space reinforced concrete frame structures with structural irregularity in plan", *Journal of Structural Engineering,* ASCE, 144(8), 04018096, https://doi.org/10.1061/(ASCE)ST.1943-541X.0002092.

Moradi, M., Tavakoli, H. and Abdollahzadeh, G.R. (2022). "Collapse probability assessment of a 4-Story RC frame under post-earthquake fire scenario", *Civil Engineering Infrastructures Journal*, 55(1), 121-137, https://doi.org/10.22059/ceij.2021.313241.1718.

Patel, S.A., Darji, A.R., Parikh, K.B. and Patel, B.R. (2016). "Fragility analysis of high-rise building structure", *Journal of Emerging Technologies and Innovative Research (JETIR)*, 3(7), 127-133.

Puppio, M.L., Pellegrino, M., Giresini, L. and Sassu, M. (2017). "Effect of material variability and mechanical eccentricity on the seismic vulnerability assessment of reinforced concrete buildings", *Buildings,* 7(3), 66, https://doi.org/10.3390/buildings7030066.

Rahnama, M. and Krawinkler, H. (1993). "Effect of soft soils and hysteresis models on seismic design spectra", Report 108(TB), The John A. Blume Earthquake Engineering Center, Stanford University, Stanford, CA.

Razmkhah, M.H., Kouhestanian, H., Shafaei, J., Pahlavan, H. and Shamekhi Amiri, M. (2021). "Probabilistic seismic assessment of moment resisting steel buildings considering soft-story and torsional irregularities", 34(11), 2476-2493, http://doi.org/10.5829/IJE.2021.34.11B.11.

Seo, J. (2018). "Seismic fragility characteristics of structural populations with irregularities", *International Journal of Computational Methods and Experimental Measurements*, 6(5), 944-954, https://doi.org/10.2495/CMEM-V6-N5-944-954.

Sharifi, N.P. and Sakulich, A.R. (2014). "Effects of eccentricity and order of vibration modes on the inelastic seismic response of 3D steel structures", In: *Active and Passive Smart Structures and Integrated Systems*, (Vol. 9057, pp. 897-903), SPIE, http://doi.org/10.1117/12.2044345.

Tavakoli, H., Moradi, M., Goodarzi, M. and Najafi, H. (2022). "Outrigger braced system placement effect on seismic collapse probability of tall buildings", *Civil Engineering Infrastructures Journal*, 20, 736-749, https://doi.org/10.1016/j.jobe.2018.09.019.

Xu, C., Deng, J., Peng, S. and Li, C. (2018). "Seismic fragility analysis of steel reinforced concrete frame structures based on different engineering demand parameters", *Journal of Building Engineering*, 20, 736-749, https://doi.org/10.1016/j.jobe.2018.09.019.

Zeng, F., Huang, Y., Zhou, J. and Bu, G. (2022). "Seismic fragility analysis and index evaluation of concrete-filled steel tube column frame-core tube structures", *Journal of Asian Architecture and Building Engineering*, 21(6), 2371-2387, https://doi.org/10.1080/13467581.2021.1972001.